Bioorganic & Medicinal Chemistry Letters 21 (2011) 1052–1056

Contents lists available at ScienceDirect

Bioorganic & Medicinal Chemistry Letters

journal homepage: www.elsevier.com/locate/bmcl

Identification of a novel small molecule targeting UQCRB of mitochondrial complex III and its anti-angiogenic activity

Hye Jin Jung [a], Ki Hyun Kim [a], Nam Doo Kim [b], Gyoonhee Han [a], Ho Jeong Kwon [a,*]

[a] Department of Biotechnology, Translational Research Center for Protein Function Control, College of Life Science and Biotechnology, Yonsei University, Seoul 120-749, Republic of Korea
[b] Drug Design Team, Equispharm Inc., 864-1, Gyeonggi, Republic of Korea

ARTICLE INFO

Article history:
Received 25 September 2010
Revised 30 November 2010
Accepted 1 December 2010
Available online 15 December 2010

Keywords:
UQCRB
Angiogenesis
O_2 sensing
HDNT

ABSTRACT

Our recent study has shown that ubiquinol-cytochrome c reductase binding protein (UQCRB), the 13.4-kDa subunit of mitochondrial complex III, plays a crucial role in hypoxia-induced angiogenesis via mitochondrial reactive oxygen species (ROS)-mediated signaling. Here we report a new synthetic small molecule targeting the mitochondrial oxygen sensor UQCRB that was identified by pharmacophore-based virtual screening and in vitro and in vivo competition binding analyses. 6-((1-Hydroxynaphthalen-4-ylamino)dioxysulfone)-2*H*-naphtho[1,8-*bc*]thiophen-2-one (HDNT) binds to the hydrophobic pocket of UQCRB and potently inhibits in vitro angiogenesis of human umbilical vein endothelial cells without cytotoxicity. Furthermore, the binding of HDNT to UQCRB suppressed mitochondrial ROS-mediated hypoxic signal transduction. These results demonstrated that HDNT is a novel synthetic small molecule targeting UQCRB and exhibits anti-angiogenic activity by modulating the oxygen-sensing function of UQCRB.

Angiogenesis is a key process for progression of many solid tumors.[1,2] Accordingly, the efficient inhibition of angiogenesis is considered to be a powerful way to suppress tumor growth and metastasis.[3,4] Consequently, several specific target proteins of angiogenesis, including vascular endothelial growth factor receptors (VEGFs), matrix metalloproteinases, aminopeptidases, histone deacetylases, and calmodulin, have been identified and anti-angiogenic agents of various scaffolds have been developed based on their inhibitory activities toward the specific targets.[5–12]

We recently isolated terpestacin, a new angiogenesis inhibitor with a unique bicyclo sesterterpene structure, from fungal metabolites.[13] To investigate the molecular mechanism of terpestacin regarding its anti-angiogenic activity, we identified a cellular binding protein of terpestacin using a reverse chemical proteomics approach. Terpestacin specifically bound to the 13.4-kDa subunit (UQCRB) of complex III in the mitochondrial respiratory chain.[14] Recent reports have suggested that reactive oxygen species (ROS) generation at mitochondrial complex III triggers hypoxia-inducible factor-1α (HIF-1α) stabilization during hypoxia.[15,16] Indeed, terpestacin binding to UQCRB inhibited hypoxia-induced ROS generation, leading to inhibition of HIF-1α and tumor angiogenesis in vivo, without disrupting mitochondrial respiration and complex III functional structure.[14] In addition, the regulation of UQCRB expression demonstrated that the protein is a critical mediator of hypoxia-induced tumor angiogenesis via mitochondrial ROS-mediated signaling.[14] This discovery suggested that small molecules targeting UQCRB in mitochondrial complex III can suppress tumor angiogenesis without acting as a respiratory poison. As such, we attempted to develop new small molecules that specifically regulate the function of UQCRB. In the present study, a novel synthetic small molecule targeting UQCRB was isolated from the smart chemical library designed by pharmacophore-based virtual screening and its anti-angiogenic activity was evaluated.

In a previous study, a docking model of terpestacin and UQCRB was constructed to elucidate the binding mode of the complex and was confirmed by surface plasmon resonance (SPR) analysis of the binding affinity of UQCRB mutants to terpestacin.[14] Consequently, docking modeling provided pharmacophores that are critical for the interaction of ligands to UQCRB. Thus, we used the pharmacophore model as a search query to identify small molecules with optimal binding property to UQCRB from a commercially available three-dimensional (3D) multi-conformer database of 3.6 million compounds (PharmoDB, Equispharm, Korea). The interaction model used for this process is characterized by these features: hydrogen bonds and lipophilic interactions. These features include hydrogen bond donors (HBDs), hydrogen bond acceptors (HBAs) and lipophilicity (lipo). Pharmacophore models were generated with the excluded volume for the heavy atoms. To account for excluded volume regions occupied by the heavy atoms in the receptor, an exclusion model is generated for the terpestacin binding site and the surrounding receptor regions. Each atom of the receptor

* Corresponding author. Tel.: +82 2 2123 5883; fax: +82 2 362 7265.
E-mail address: kwonhj@yonsei.ac.kr (H.J. Kwon).

0960-894X/$ - see front matter © 2010 Elsevier Ltd. All rights reserved.
doi:10.1016/j.bmcl.2010.12.002

selected for inclusion in the model is represented as an exclusion point. We performed this procedure by using SBF (structure-based focusing) module in Cerius2 (Accelrys, San Diego, USA). Among the virtual screening hit compounds, those that exhibited unfavorable interactions with the binding site or unrealistic conformations were filtered out by visual inspection. Finally, we selected 150 compounds for in vitro and in vivo competition binding analyses with UQCRB.

The activity of the 150 virtually screened compounds was evaluated through three types of in vitro and in vivo competitive binding assays based on phage display, fluorescence staining, and SPR as described previously.[14] Several hit compounds were found to significantly bind to UQCRB from all competitive binding analyses. We identified 6-((1-hydroxynaphthalen-4-ylamino)-dioxysulfone)-2*H*-naphtho[1,8-*bc*]thiophen-2-one (HDNT) from the virtually screened compound library as a new synthetic small molecule targeting UQCRB with the highest binding affinity (Fig. 1a). To further elucidate the interaction between HDNT and UQCRB, a molecular docking study was performed with the results presented in Figure 1b.[17–19] The docking model revealed that HDNT was bound to UQCRB via hydrogen bonding interactions with Thr 37, Arg 59, and Leu 67 residues of UQCRB. The 4-hydroxy-naphthalene moiety (A) of HDNT was involved in a hydrophobic interaction with non-aromatic residues of the side chains of Leu 67, Ile 63, and Leu 30 in UQCRB. In addition, the 2*H*-naphtho [1,8-*bc*]thiophen-2-one (B) moiety of HDNT was involved in a pi–pi interaction with the aromatic residue of Tyr 39 in UQCRB. By analyzing the results of the docking studies, we found that HDNT structurally overlapped with terpestacin in the UQCRB docking model (Fig. 1c).[14]

To confirm the specific binding of HDNT to UQCRB, a phage display-based competitive binding assay was first performed using T7 bacteriophages expressing UQCRB.[20] Biotin did not bind to UQCRB-encoding phages, whereas biotinylated terpestacin (BT), which binds to UQCRB, specifically bound to UQCRB-encoding phages (Fig. 2a). However, the binding of UQCRB-encoding phages to BT was markedly inhibited in the presence of excess free terpestacin. HDNT also significantly blocked the interaction between BT and UQCRB-phages, implying that HDNT binds to UQCRB. Next, the interaction between HDNT and UQCRB at the cellular level was assessed by competitive binding analysis using ter-coumarin, a fluorescent probe for terpestacin.[21] Treatment of human umbilical vein endothelial cells (HUVECs) with ter-coumarin resulted in intense blue fluorescence in the cytoplasmic area where mitochondria are present, unlike with coumarin treatment (Fig. 2b). When HUVECs were pretreated with terpestacin, binding between ter-coumarin and UQCRB was inhibited by the competitive binding of terpestacin to UQCRB in the cells, resulting in a significant decrease in the fluorescence intensity of ter-coumarin. Pretreatment with HDNT also decreased the fluorescence intensity of ter-coumarin to the same extent as terpestacin, indicating that HDNT binds to UQCRB in the cells. To further demonstrate the binding of HDNT to UQCRB, we performed SPR (BIAcore) analysis.[22] Control biotin and BT were sequentially immobilized onto the surface of a streptavidin-coated sensor chip and the apparent binding affinities were calculated by subtraction of resonance values of UQCRB binding to control biotin from those of UQCRB binding to BT. For competitive binding analyses, terpestacin and HDNT were each incubated with UQCRB protein, and then the complexes were injected into flow cells of the sensor chip. Consequently, the binding efficiency of UQCRB to BT was decreased to 40% and 60% by the preincubation of terpestacin and HDNT each with UQCRB protein, confirming that HDNT directly binds to UQCRB (Fig. 2c). Together, the in vitro and in vivo competitive binding data clearly demonstrated that HDNT is a novel synthetic small molecule targeting UQCRB.

To evaluate whether binding of HDNT to UQCRB affects mitochondrial function, the effect of HDNT on the mitochondrial

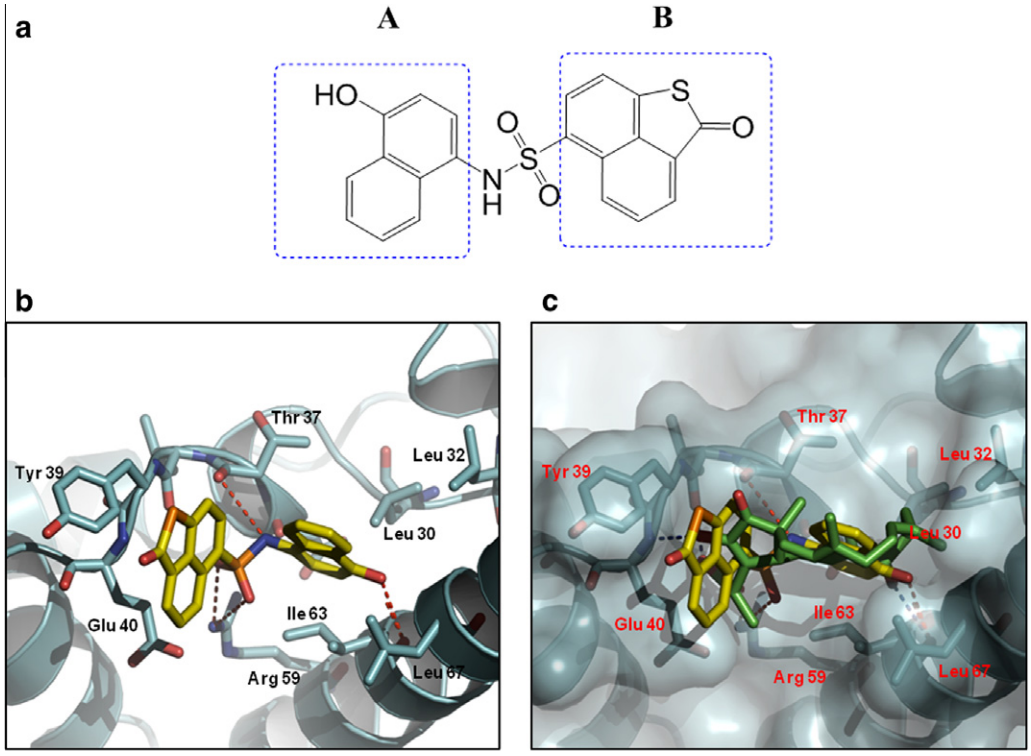

Figure 1. Docking model of the HDNT–UQCRB complex. (a) The structure of HDNT. (b) The docking model of HDNT to UQCRB obtained from the AutoDock4 program. Red dotted lines represent hydrogen bonds between HDNT and UQCRB. (c) Comparison of the proposed binding model of HDNT and terpestacin. HDNT is indicated in yellow and terpestacin in green. The blue dotted lines represent hydrogen bonds between terpestacin and UQCRB. A terpestacin binding model was derived from AutoDock program used in our previous study.[14]

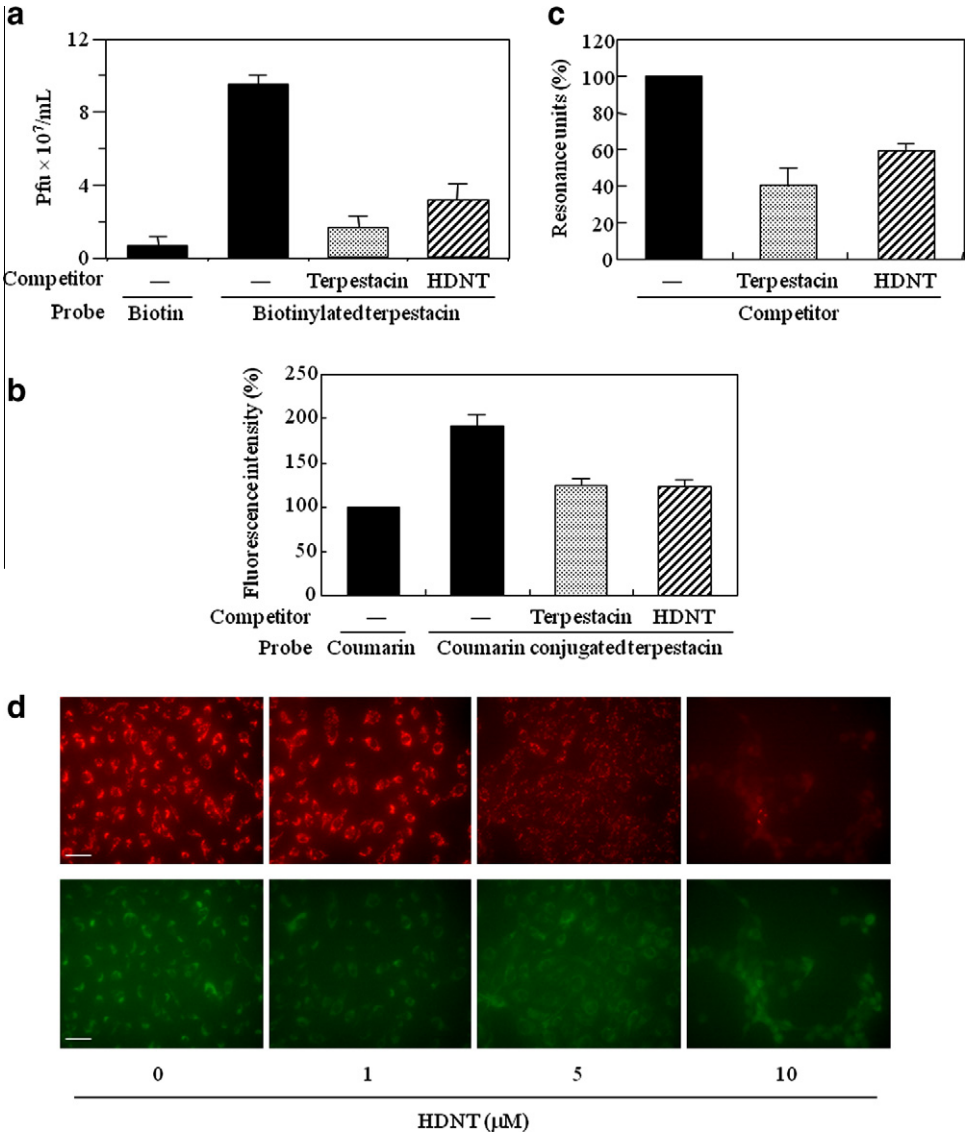

Figure 2. Analysis of the interaction between HDNT and UQCRB. (a) Effect of HDNT on the binding between UQCRB-phages and immobilized terpestacin. (b) Effect of HDNT on the binding of ter-coumarin to UQCRB in HUVECs. (c) Effect of HDNT on the interaction between purified UQCRB protein and immobilized terpestacin by SPR analysis. (d) Effect of HDNT on the mitochondrial membrane potential. HUVECs were incubated for 4 h with HDNT and then stained with 0.25 μg/mL of JC-1 (mitochondrial membrane potential marker) for 15 min. Fluorescence images were obtained using a fluorescence microscope. *Scale bar*, 200 μm.

membrane potential of HUVECs was measured using the JC-1 fluorescent marker. Treatment with HDNT dose-dependently led to a decrease in red fluorescence and an increase in green fluorescence, indicating that HDNT causes a loss of the mitochondrial membrane potential by targeting UQCRB (Fig. 2d).

From the results above, we found that HDNT obviously regulates the function of UQCRB in mitochondrial complex III. Our previous study had shown that UQCRB plays a crucial role in tumor angiogenesis and, terpestacin, the first natural small molecule targeting UQCRB, exhibits potent anti-angiogenic activity.[14] To explore the anti-angiogenic activity of HDNT, we first investigated the effect of HDNT on the growth of various cell lines including HUVECs using the MTT colorimetric assay. As shown in Table 1, HDNT potently inhibited the proliferation of HUVECs with an IC_{50} of 1 μM. Notably, HDNT selectively inhibited the growth of HUVECs than that of cancer cell lines (human fibrosarcoma HT1080, human cervical carcinoma HeLa, human hepatoma HepG2). These data indicate that HDNT may exhibit the anti-angiogenic activity by specific inhibition of endothelial cell growth. We next investigated the effect of HDNT on several angiogenic phenotypes of endothelial cells such as cell invasion and tube formation. Serum-starved HUVECs were stimulated by VEGF with or without HDNT, and in vitro angiogenesis assays were performed.[23] HDNT suppressed VEGF-induced invasion and tube formation of HUVECs in a dose-dependent manner without affecting endothelial cell viability (Fig. 3). These data demonstrate that HDNT is a new anti-angiogenic agent targeting UQCRB.

Table 1
IC_{50} values of HDNT on various cell lines

Cell lines	HUVEC	HT1080	HeLa	HepG2
IC_{50} (μM)	1	20	20	20

The increase in complex III-derived ROS generation during hypoxia triggers HIF-1α stabilization and consequently mediates the expression of its target genes such as *VEGF*.[15,16] UQCRB is a key component in mitochondrial complex III and acts as an O_2

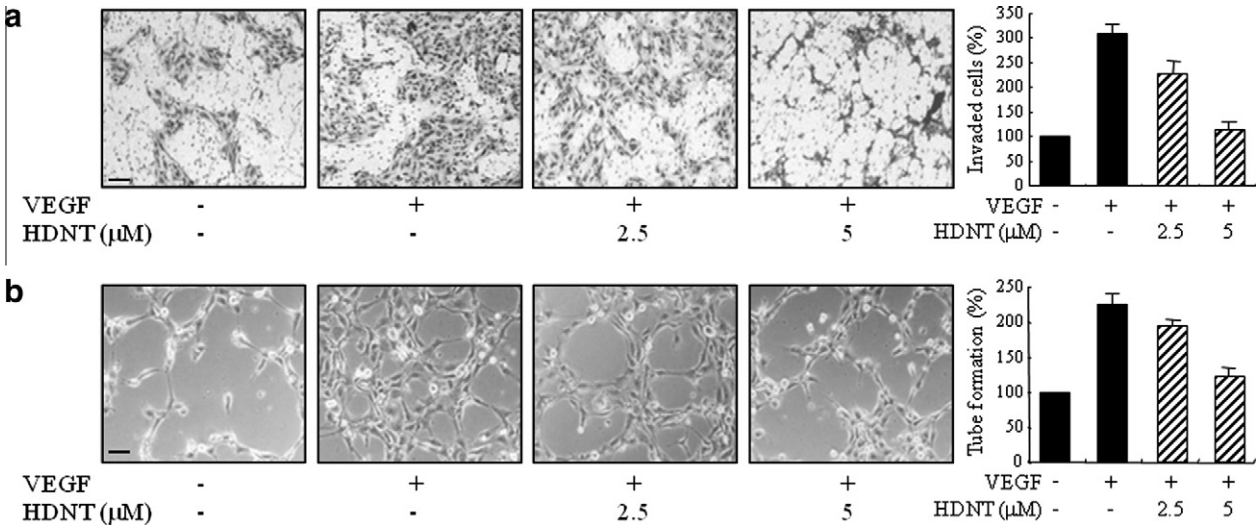

Figure 3. Effect of HDNT on in vitro angiogenesis. Serum-starved HUVECs were stimulated with VEGF (30 ng/mL) in the presence or absence of HDNT. (a) Inhibitory activity of HDNT on endothelial cell invasion. (b) Effect of HDNT on tube forming ability of HUVECs. *Scale bar*, 200 μm.

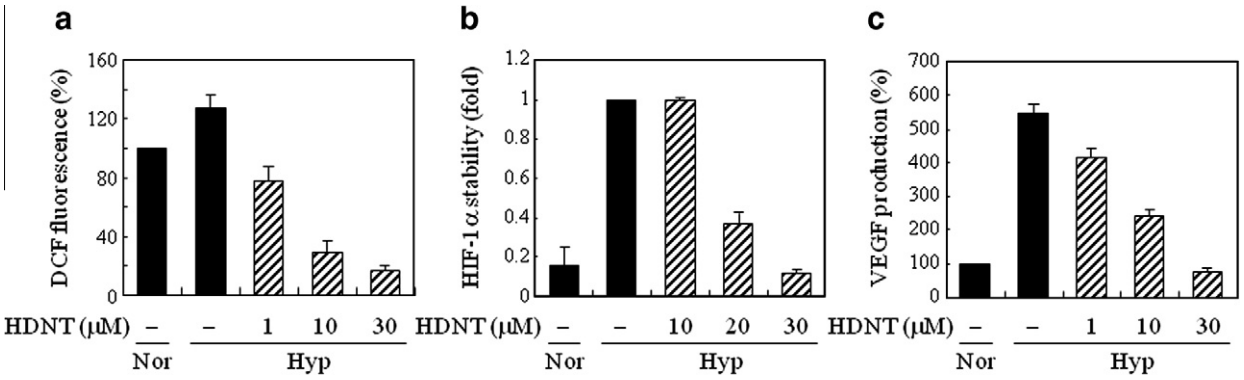

Figure 4. Regulation of mitochondrial ROS-mediated hypoxic signal transduction by HDNT. (a) Effect of HDNT on mitochondrial ROS generation. Intracellular ROS levels were determined by the DCF fluorescence. HepG2 cells were pretreated with HDNT for 30 min and then exposed to 1% O_2 for 10 min. *Nor*, normoxia; *Hyp*, hypoxia. (b) Effect of HDNT on HIF-1α stability. HIF-1α protein levels were analyzed using western blot analysis. HepG2 cells were pretreated with HDNT for 30 min and then exposed to 1% O_2 for 4 h. Western blot data were quantitated using densitometry. (c) Effect of HDNT on VEGF expression. HepG2 cells were pretreated with HDNT for 30 min and then exposed to 1% O_2 for 16 h. The concentration of VEGF protein in the culture supernatant was determined using an ELISA specific for VEGF.

sensor, thereby mediating hypoxia-induced tumor angiogenesis.[14] To determine whether the anti-angiogenic activity of HDNT is associated with the regulation of UQCRB function in O_2 sensing, we examined the effect of HDNT on mitochondrial ROS-mediated hypoxic signal transduction progression. HDNT dose-dependently suppressed hypoxia-induced mitochondrial ROS generation in HepG2 hepatoma cells (Fig. 4a). Moreover, the compound markedly inhibited HIF-1α accumulation and VEGF expression induced by hypoxia (Fig. 4b and c). These results suggested that the anti-angiogenic activity of HDNT is related to the modulation of the O_2 sensing function of UQCRB.

In conclusion, a new synthetic small molecule that can regulate the function of UQCRB has been identified through a reverse chemical genetics approach. The specific binding of HDNT to UQCRB was demonstrated by in vitro and in vivo competitive binding assays. HDNT also exhibited considerable anti-angiogenic activity without cytotoxicity by regulating the O_2 sensing function of UQCRB. However, HDNT reduced the basal ROS as well as the mitochondrial ROS induced by hypoxia. Recent evidence has revealed that the membrane potential enhances the formation of superoxide from Complex III by opposing electron transfer from heme b_L to b_H.[24] Treatment with HDNT during normoxia decreased the mitochondrial membrane potential by targeting UQCRB (Fig. 2d). These results indicate that the reduction of mitochondrial ROS generation below the basal level by HDNT might correlate with the lowered membrane potential. Nonetheless, HDNT did not affect cell viability at the effective concentrations for the inhibition of mitochondrial ROS generation. Notably, the anti-angiogenic potential of HDNT in vitro (IC_{50} = 5 μM) was five times stronger than that of terpestacin (IC_{50} = 25 μM), the original natural small molecule targeting UQCRB.[13,14] However, HDNT still exhibits biological activity in the micromolar range and has relatively low solubility in water. Thus, a further lead optimization study will be required to improve the pharmacological potential of HDNT. In addition, we cannot exclude the possibility that the anti-angiogenic activity of HDNT may result from the multiple regulation of other cellular proteins, as well as UQCRB itself, because small molecules can bind to more than one protein. However, HDNT clearly belongs to a new class of anti-angiogenic agents that targets UQCRB, and can serve as a valuable probe to explore the role of UQCRB in angiogenesis. Moreover, the present study supports the idea that UQCRB is a promising target for anti-angiogenic and anti-tumor drug development.

Acknowledgments

This work was supported by grants from the National Research Foundation of Korea Grant funded by the Korean Government (MEST) (2009-0092964 and 2010-0017984), the Translational

Research Center for Protein Function Control, NRF (2009-0083522), the National R&D Program for Cancer Control (0620350), Ministry of Health & Welfare, and from the Brain Korea 21 project, Republic of Korea.

References and notes

1. Hanahan, D.; Folkman, J. *Cell* **1996**, *86*, 353.
2. Andre, T.; Chastre, E.; Kotelevets, L.; Vaillant, J. C.; Louvet, C.; Balosso, J.; Gall, E. L.; Prevot, S.; Gespach, C. *Rev. Med. Interne* **1998**, *19*, 904.
3. Folkman, J. *Semin. Oncol.* **2001**, *28*, 536.
4. Carmeliet, P.; Jain, R. K. *Nature* **2000**, *407*, 249.
5. Millauer, B.; Wizigmann-Voos, S.; Schnürch, H.; Martinez, R.; Møller, N. P.; Risau, W.; Ullrich, A. *Cell* **1993**, *72*, 835.
6. Huang, D.; Ding, Y.; Li, Y.; Luo, W. M.; Zhang, Z. F.; Snider, J.; Vandenbeldt, K.; Qian, C. N.; Teh, B. T. *Cancer Res.* **2010**, *70*, 1053.
7. Moses, M. A.; Langer, R. *J. Cell. Biochem.* **1991**, *47*, 230.
8. Sin, N.; Meng, L.; Wang, M. Q.; Wen, J. J.; Bornmann, W. G.; Crews, C. M. *Proc. Natl. Acad. Sci. U.S.A.* **1997**, *94*, 6099.
9. Lee, J.; Shim, J. S.; Jung, S. A.; Lee, S. T.; Kwon, H. J. *Bioorg. Med. Chem. Lett.* **2005**, *15*, 181.
10. Kim, M. S.; Kwon, H. J.; Lee, Y. M.; Baek, J. H.; Jang, J. E.; Lee, S. W.; Moon, E. J.; Kim, H. S.; Lee, S. K.; Chung, H. Y.; Kim, C. W.; Kim, K. W. *Nat. Med.* **2001**, *7*, 437.
11. Kwon, H. J.; Kim, M. S.; Kim, M. J.; Nakajima, H.; Kim, K. W. *Int. J. Cancer* **2002**, *97*, 290.
12. Jung, H. J.; Kim, J. H.; Shim, J. S.; Kwon, H. J. *J. Biol. Chem.* **2010**, *285*, 25867.
13. Jung, H. J.; Lee, H. B.; Kim, C. J.; Rho, J. R.; Shin, J.; Kwon, H. J. *J. Antibiot. (Tokyo)* **2003**, *56*, 492.
14. Jung, H. J.; Shim, J. S.; Lee, J.; Song, Y. M.; Park, K. C.; Choi, S. H.; Kim, N. D.; Yoon, J. H.; Mungai, P. T.; Schumacker, P. T.; Kwon, H. J. *J. Biol. Chem.* **2010**, *285*, 11584.
15. Chandel, N. S.; Maltepe, E.; Goldwasser, E.; Mathieu, C. E.; Simon, M. C.; Schumacker, P. T. *Proc. Natl. Acad. Sci. U.S.A.* **1998**, *95*, 11715.
16. Brunelle, J. K.; Bell, E. L.; Quesada, N. M.; Vercauteren, K.; Tiranti, V.; Zeviani, M.; Scarpulla, R. C.; Chandel, N. S. *Cell Metab.* **2005**, *1*, 409.
17. For the refined docking model of HDNT to UQCRB, automated docking simulation was performed using AutoDock4.[18] The X-ray crystal structure of UQCRB from Protein Data Bank (PDB code 3BCC) was used for our docking simulation.[19] For the docking, the structure of UQCRB was kept rigid whereas all torsional bonds in HDNT were set free to perform flexible docking. The binding energy between protein and inhibitors was evaluated using atom affinity potentials that were pre-calculated on grid maps using AutoGrid. The grid maps had dimensions of $40 \times 40 \times 40$ Å with 0.375-Å spacings between grid points. In AutoDock4, docking was performed by combining a global genetic algorithm (Lamarckian genetic algorithm) with local minimization. A total of 100 trials were performed for each docking, and final docked conformations were clustered using a tolerance of 1 Å root-mean-square deviation (RMSD). The molecular graphics of selected possible docking models with HDNT was generated using the PyMol package (http://www.pymol.org).
18. Morris, G. M.; Huey, R.; Lindstrom, W.; Sanner, M. F.; Belew, R. K.; Goodsell, D. S.; Olson, A. J. *J. Comput. Chem.* **2009**, *30*, 2785.
19. Zhang, Z.; Huang, L.; Shulmeister, V. M.; Chi, Y. I.; Kim, K. K.; Hung, L. W.; Crofts, A. R.; Berry, E. A.; Kim, S. H. *Nature* **1998**, *392*, 677.
20. Competitive binding assay by phage display: biotin and biotinylated terpestacin diluted in Tris-buffered saline (TBS, pH 7.5) were immobilized on a streptavidin-coated well plate (Pierce Biotechnology), each at a concentration of 10 μM. UQCRB-encoding T7 phages were diluted in TBS (1×10^7 pfu/mL) and added to the terpestacin-immobilized wells in the presence or absence of competitors (100 μM). After incubation for 1 h at room temperature with gentle shaking, the well plate was washed with TBS and bound phage particles were eluted with 100 μM terpestacin diluted in TBS. The binding phages were infected into the *Escherichia coli* strain BLT5615 grown on Luria–Bertani (LB) agar plates supplemented with 50 μg/mL ampicillin, and then the plaques were counted to calculate plaque forming units (pfus).
21. Competitive binding assay by fluorescence staining: HUVECs were incubated with 20 μM coumarin or coumarin-conjugated terpestacin (ter-coumarin) for 24 h in the presence or absence of competitors (10 μM HDNT or 30 μM terpestacin). After washing with phosphate-buffered saline (PBS, pH 7.4), cells were observed under a fluorescence microscope (Olympus). The fluorescence intensity was measured using an FL600 microplate fluorescence reader (Bio-Tek).
22. Competitive binding assay by SPR: Biotin and biotinylated terpestacin were sequentially immobilized onto the surface of a streptavidin-coated sensor chip. Competitors (25 μM) were incubated with purified UQCRB protein (25 μM) in the running buffer (10 mM HEPES, 150 mM NaCl, 3 mM EDTA (pH 7.4)), and then UQCRB–competitor complexes were injected onto the sensor chip at a flow rate of 30 μL/min. The surface of the sensor chip was regenerated by injection of 5 μL of the regeneration buffer (50 mM NaOH). Molecular interaction analysis was performed using the BIAcore 2000 system (BIAcore AB) and the apparent binding affinities were calculated by subtraction of resonance values of UQCRB binding to control biotin from those of UQCRB binding to biotinylated terpestacin.
23. In vitro angiogenesis assays: the invasiveness of HUVECs was examined using a Transwell chamber system with 8.0-μm pore-sized polycarbonate filter inserts (Corning Costar) as described previously.[13] The total number of invaded cells was counted using an optical microscope at a 100× magnification. The tube formation assay was performed using HUVECs grown on Matrigel (Collaborative Biomedical Products) as described previously.[13] Tube formation was quantified by counting the number of connected cells in randomly selected fields at a 100× magnification and dividing that number by the total number of cells in the same field.
24. Rottenberg, H.; Covian, R.; Trumpower, B. L. *J. Biol. Chem.* **2009**, *284*, 19203.